Edinburgh Research Explorer

Enhancing fracture toughness of carbon fiber/epoxy composites using polyphenylene ether as a modifier

Enhancing fracture toughness of carbon fiber/epoxy composites using polyphenylene ether as a modifier

Naveen Veeramani[1,2]*, Machar Devine[2], James A Quinn[2],

Arun Kumar Alapati[2], Alp Bolluk[2], Dipa Ray[2]

1. National Aerospace Laboratories,
    Council of Scientific and Industrial Research (CSIR-NAL),
    Bangalore – India.
    Email: naveen.v@nal.res.in
    Visiting Researcher: University of Edinburgh, United Kingdom

2. School of Engineering, Institute for Materials and Processes, The University of Edinburgh, Sanderson Building, Robert Stevenson Road, Edinburgh, EH9 3FB, Scotland, United Kingdom
    *Corresponding Author Email: naveen.v@nal.res.in

Abstract

In this study, carbon fiber/epoxy composites (CFRP) were fabricated by vacuum-assisted resin infusion moulding (VARIM) with polyphenylene ether (PPE) as a toughening agent. The PPE contained hydroxyl end groups that facilitated chemical bonding with epoxy during curing. PPE was incorporated into the epoxy matrix by dissolution, and spreading in the interlaminar regions. The presence of PPE as a toughener exhibited significant improvement in the Mode-I fracture toughness of the composites. The CFRP samples, which were toughened with 5 wt.% and 10 wt.% PPE, showed about 191% to 380% enhancement, respectively, in the critical energy release rate (G_{IC}) compared to the unmodified sample. Dynamic mechanical analysis (DMA) showed about a 6°C increase in the glass transition temperature of the toughened composites, which is an interesting aspect of this work. These results indicate the potential of using PPE as a toughening agent in CFRP composites.

Keywords: Epoxy, carbon fiber, resin infusion, polyphenylene ether, toughener, composites, Mode-I fracture toughness

1 Introduction

The usage of carbon fiber-reinforced polymer (CFRP) composites is rapidly increasing with time in various applications. CFRP composites are extensively used in aerospace, automobiles, windmills, sports goods, and other structural applications, due to their superior properties such as high specific strength, high stiffness, chemical resistance, and durability in corrosive environments [1−3]. The global CFRP demand is estimated to be a massive 285 thousand metric tons by the end of 2025 [4]. This is mainly attributed to the worldwide effort by many countries to reduce CO_2 emissions and the huge consumption of CFRP for renewable energy through windmills, tidal blades, and solar panels. In addition to the superior properties of carbon fiber, research on low-cost carbon fiber will increase the consumption of CFRP further in the coming years.

The fiber reinforcement, resin, and its cure kinetics control the final properties of the composites. Determining an optimum cure cycle for a resin system is critical, as it directly influences the mechanical properties of the composites [5]. For example, high-temperature cured epoxies and other resins are mainly targeted for aerospace applications [6, 7]. Room-temperature cured epoxy resins are also widely used for various applications, such as manufacturing wind turbine blades, adhesives, insulators, and civil structures. However, epoxy resin composites are generally brittle in nature, and there are several ways to increase their fracture toughness. Quan et al., [8] reported a 63% improvement in fracture toughness for a room-temperature cured epoxy system modified with in-situ nanofibers of polyphenylene oxide (PPO) oligomer through an interpenetrating polymer network formation. In recent times, the incorporation of thermoplastic additives into CFRP composites has become a focus of interest in the field of polymer composites. Thermoplastic additives, or nanofillers, are added to the matrix mainly to improve the fracture toughness or thermal properties of the CFRP [9, 10]. There are various thermoplastic polymers, such as polyamide, polyimide, polyether sulfone [11], and polyphenylene ether (PPE), that can be added to CFRP composites to tailor their properties. Daelemans et al., [12] reported a 45% increase in Mode-I interlaminar fracture toughness for CF/epoxy composites toughened with electrospun polyamide nanofibrous veils. An improvement of 61.5% in Mode-I fracture toughness was reported by Chen et al., [13] for CF/epoxy composites toughened with porous films of polyether sulphone (PES) by the interleaving method.

Chen et al., [14] reported a combination of extrinsic and intrinsic multiscale toughening mechanisms to improve the interlaminar fracture toughness of CFRP composites. The addition of a toughening system consisting of nanoscale core-shell rubber (CSR) and microscale short carbon fiber (SCF) was found to increase the fracture toughness of CFRP composites by 127% compared to the unmodified sample. While the fracture toughness is improved, there is an adverse effect of a reduction in tensile properties in some composites. Luo et al., [15] reported a tensile strength reduction from 64.9 MPa to 52.6 MPa for a diglycidyl ether of bisphenol-A (DGEBA)/fluoro-terminated hyperbranched poly(phenylene oxide) (FHPPO; 20 wt.%) composite, and Lv et al., [16] reported that the tensile strength of DGEBA modified with epoxidized hyperbranched poly(phenylene oxide; EHPPO) increased from 70 MPa (unmodified sample) to 90 MPa with 10 wt.% EHPPO and then decreased to 85 MPa when the EHPPO content was increased further to 20 wt.%. Nguyen et al., [17] compared the performance of two types of poly(2,6-dimethyl-1,4-phenylene ether) (PPE) as toughening agents of epoxy/ionic liquid networks. The critical stress intensity fracture toughness (K_{IC}) improved by 150% and 200%, respectively, in the modified samples.

There are only a few literature reports on the incorporation of PPE into CFRP composites. Bisphenol-A epoxy resin and PPE-based molecular composites with in-situ reinforcement were reported by Guan et al., [18]. The composite samples showed a 73°C increase in glass transition temperature (156°C−229°C) 60% improvement in fracture toughness (K_{IC}; 1.1 to 1.79 MPa.m$^{1/2}$), a 30% improvement in tensile strength (30 to 39 MPa), and a 55% increase in elongation at break (0.9 to 1.4%) with respect to the reference sample. Huang et al., [19] developed carbon fiber prepregs (8+8 layers) and epoxy-based composites, toughened with PPE particles by interleaving at the midplane. The composite samples containing 10 wt.% of PPE exhibited a 65% improvement in Mode-I interlaminar fracture toughness (G_{IC}). In addition to increasing fracture toughness, PPE is also known for its excellent electrical properties. Weng et al., [20] reported an epoxy system modified with polyphenylene oxide (PPO) for the production of high-frequency copper claddings for electrical applications. The modified epoxy laminates with 20 wt.% PPO has shown a considerable reduction in dielectric constant and dielectric loss, with the lowest values of 3.76/10^7 Hz and 2.11×10^{-3} /10^7 Hz, respectively.

In this experimental study, carbon fiber-epoxy composites incorporated with PPE toughener were fabricated by the liquid resin infusion method. The PPE particles were added to the epoxy matrix by two methods: dissolution and interleaving. In the dissolution method, the known quantity of PPE particles was mixed into the resin by manual stirring before the resin infusion process. In the interleaving method, the PPE particles were sprinkled over the CF layers, followed by resin infusion. The effect of PPE toughener on the glass transition temperature and mechanical properties of the composites was studied. The viscoelastic properties of the laminates, before and after modification with PPE, were measured with the dynamic mechanical analyzer. The Mode-I fracture toughness was studied using the Double Cantilever Beam (DCB) test.

2 Experimental

2.1 Materials

Epoxy resin (IN 2), hardener (AT 30), and other consumables required for the resin infusion process, such as resin infusion mesh, spiral tubes for resin distribution, silicon ports, vacuum tubes, and vacuum bagging films, were purchased from Easy Composites Ltd. U.K. The unidirectional (0°) carbon fabric with an aerial weight of 603 GSM was procured from SAERTEX Group in Germany. A free sample of PPE (NORYL^{TM} SA-90 Resin; Hydroxy Eq.wt. = 840 g/mol; Mn = 1600) was supplied by SABIC. Coupons for the double cantilever beam (DCB) test was made by inserting a thin (13 µm) release film of perfluoroalkoxy alkane to form a pre-crack length of 63 mm for initiating delamination (ASTM D5528).

2.2 Fabrication methods

Carbon fiber/epoxy composites were manufactured using vacuum-assisted resin infusion moulding (VARIM). Four layers of carbon fabric each with a dimension of (450 mm × 450 mm × 0.8 mm), were cut into squares and stacked together on a glass mould. A measured quantity of finely ground PPE powder was added to the epoxy resin, dissolved by hand stirring, and then a hardener was added. A PPE concentration of 5 wt.% and 10 wt.% were used for CFRP samples prepared by the dissolution method, and 5 wt.% of PPE was used for samples made by the interleaving method. With 5 wt.% of PPE addition, the resin mixture was homogeneous, and the resin infusion process was smooth. Whereas, when 10 wt.% of PPE was added, the resin mixture looked slightly heterogeneous with increased viscosity, but the

infusion process was still possible. The formulated resin mixture was then infused into the CF fabrics under a controlled vacuum. In the case of interleaving, 5 wt.% of PPE powder was divided into three equal quantities for uniform distribution among the three interlaminar regions formed by the stack of four CF layers. A pre-crack release film was inserted at the midplane between the 2nd and 3rd CF layers to prepare DCB specimens for the Mode-I interlaminar fracture toughness test. Figure 1 shows the schematic diagram for fabricating the CFRP composites.
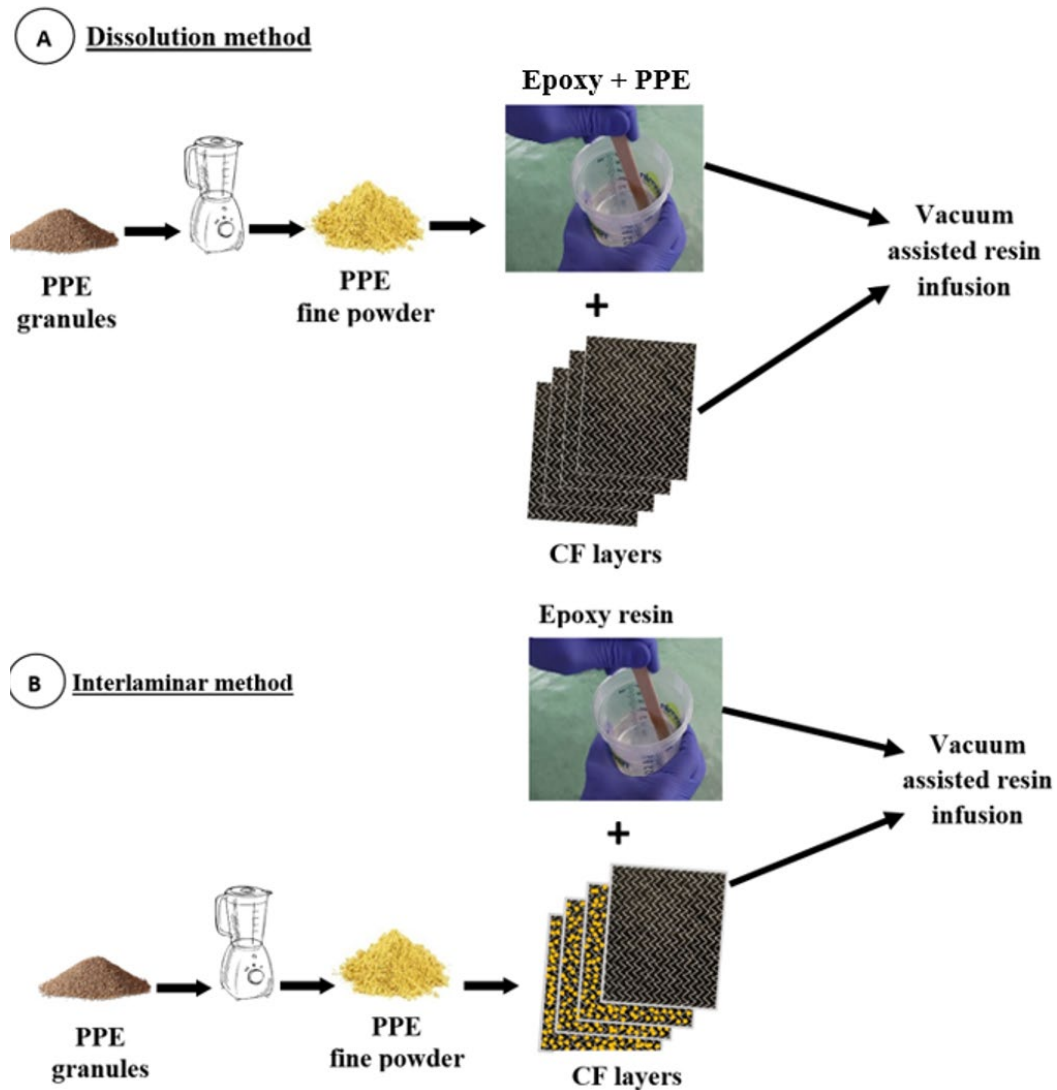

Figure 1. Schematic diagram of the fabrication of CFRP composites: **A**. PPE addition by dissolution method; **B**. PPE addition by interleaving method.

In this study, four different composites were prepared with different PPE concentration as;

1. **CF/Ep**: CF/Epoxy without any additive (unmodified; reference sample).
2. **CF/Ep/PPE5-D**: Addition of 5 wt.% of PPE in epoxy by dissolution.

3. **CF/Ep/PPE5-I**: Addition of 5 wt.% of PPE in between CF layers (Interleaving).
4. **CF/Ep/PPE10-D**: Addition of 10 wt.% of PPE in epoxy by dissolution.

The method of PPE addition during composite fabrication is shown in Figure 2.
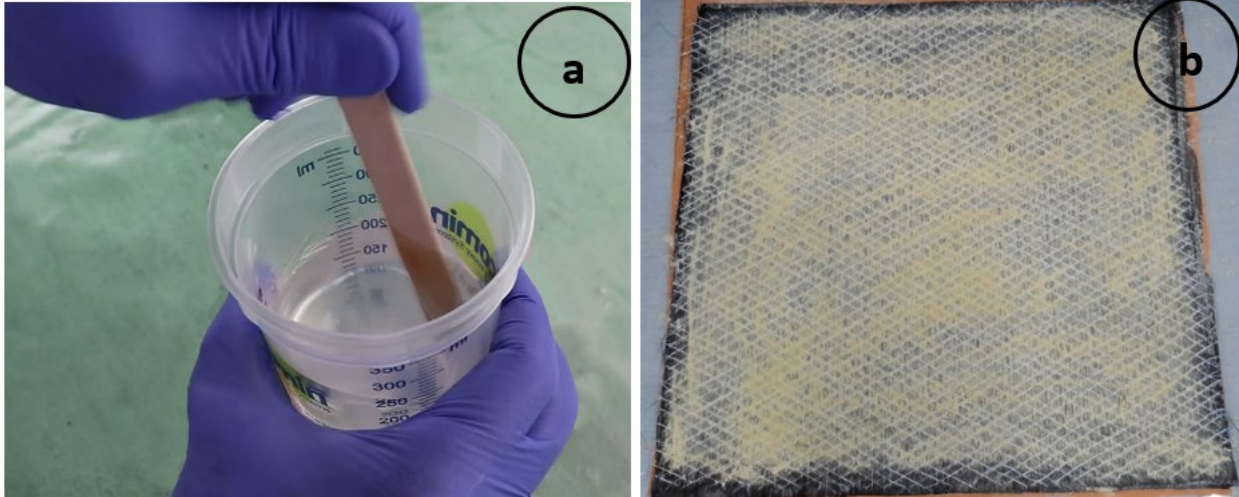

Figure 2. Addition of PPE particles by (a) Dissolution and (b) Interleaving methods (450 mm × 450 mm × 0.8 mm carbon fabric layers).

When the PPE concentration was increased from 5 wt.% to 10 wt.%, the resin mixture became considerably viscous, and the infusion process took more time to complete (from 8 minutes to 13 minutes). Hence, 5 wt.% PPE addition was found to be the optimum quantity for easy infusion processing. The typical vacuum-assisted resin infusion process is shown in Figure 3.
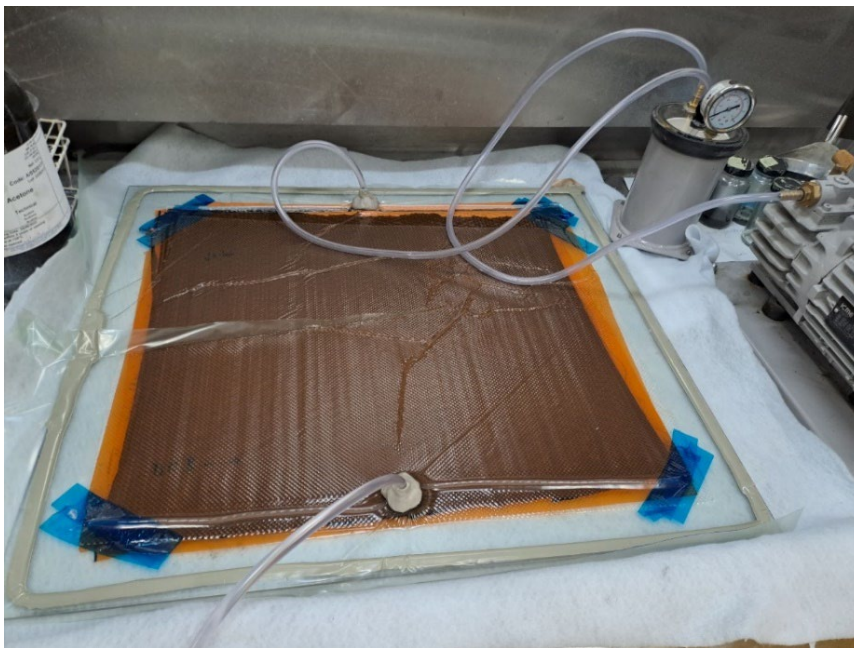

Figure 3. Vacuum-assisted resin infusion moulding (VARIM) process.

2.3 Testing

The laminates were cut into test specimens of the required dimensions in a diamond-tipped wet saw cutter machine (RAMG-1011). Test specimens of the required length, breadth, and thickness (60 mm; 12 mm, and 3 mm, respectively) were extracted as per the ASTM standard (D 4065) for dynamic mechanical analysis (DMA 850; TA Instruments, USA). The tensile test specimens were cut into 250mm × 15mm × 3mm coupons as per ASTM D3039 standards. Double cantilever beam (DCB) test specimens were extracted as 125 mm × 25 mm ×3 mm as per ASTM D5528. Small samples of composite specimens were mounted in epoxy resin with the cross-section side facing upwards. These samples were polished in a polisher (ATA Saphir 520, Germany) using different abrasives in a 15-minute sequence each. The polished samples were subjected to gold sputter coating before examination under the scanning electron microscope (ZEISS, Germany).

The solubility of PPE in epoxy and the curing of liquid epoxy resin with different PPE contents and hardeners were monitored *in situ* under an optical microscope (ZEISS Axioskop 2; ×5, Germany) to investigate the PPE phase in the cured resin and the presence of micro-voids, if any. Finely ground PPE particles were mixed with epoxy resin at different concentrations (2.5, 5, and 10 wt.%). In the cases of 2.5 wt.% and 5 wt.%, the PPE was dissolved in epoxy resin, and the infusion process was quite normal. However, when wt.10% was tried, the dissolution of PPE was found to be difficult as it crossed the dissolution limit. A few PPE particles were found to be suspended in the resin; the viscosity of the mixture increased, but the infusion was still possible. Hence, 5 wt.% of PPW was found to be the optimum quantity. The fiber volume fraction of the composite was measured through the resin burn-off method in a muffle furnace (Thermal Engineering Services, Bangalore−India) as per ASTM D3171.

The glass transition temperature was measured in a dynamic mechanical analyzer (TA Instruments, USA; DMA 850) from room temperature to 180°C at a heating rate of 3°C/min. The frequency was 1 Hz, and the dynamic deformation was maintained at 10 μm. The density of the composite samples was measured by the water displacement method (ASTM D792) using a density measurement kit (OHAUS Adventurer Density Kit, USA). The tensile properties of the samples were tested in a servo-hydraulic test machine (INSTRON 8802, USA; 250 kN) at a loading rate of 2 mm/min. Interlaminar fracture toughness (Mode-I G_{IC}) of the DCB specimens was tested in a universal testing machine (UTM, INSTRON 3369, USA; 10 kN) at a loading rate of 3 mm/min, with a digital image correlation (IMETRUM DIC, Bristol,

UK) for crack length measurement. The G_{IC} values were calculated by modified beam theory (MBT) as per ASTM D-5528. Cross-sectional analysis of the mounted samples was done with an SEM (ZEISS, Germany) at 10 kV.

3 Results and discussion

3.1 Optical microscopy

Optical microscopy images of epoxy resin dissolved with varying amounts of PPE powder are shown in Figure 4. As expected, the neat epoxy sample (Figure 4a) was observed to be homogeneous. Figure 4b shows a cured epoxy sample dissolved with 5 wt.% of PPE, which was also fairly homogeneous. When 10 wt.% of PPE was added with epoxy (Figure 4c), the dissolution was not complete and the mixture was not homogeneous. The mixture became more viscous and started forming a few lumps of PPE particles. Therefore, the resin mixture needed relatively vigorous stirring, which allowed air bubbles to enter the mixture, creating micro-voids. This phase separation suggests that 5 wt.% of PPE is an optimum quantity for dissolution into the epoxy resin.
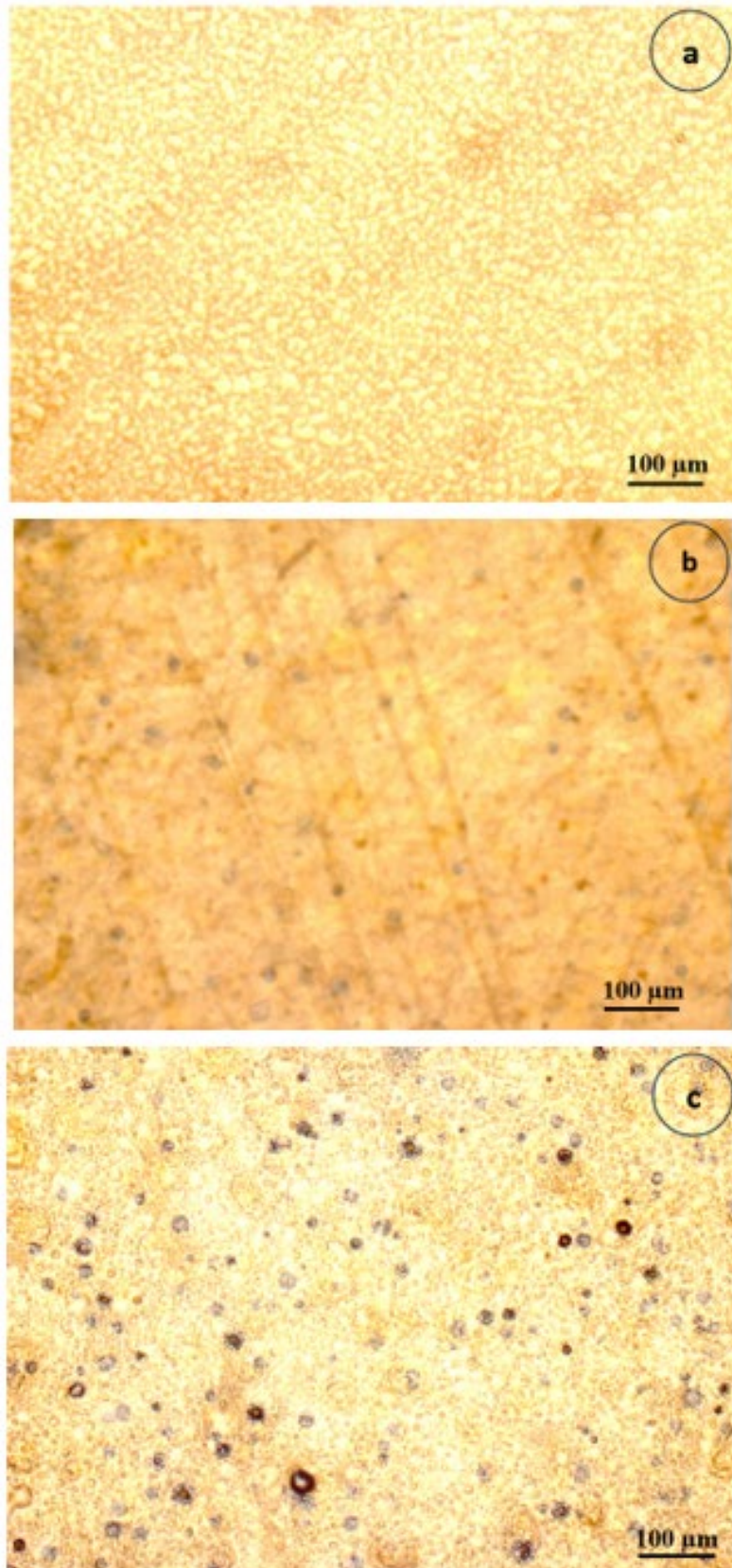
Figure 4: Optical micrographs of **a.** Neat epoxy; **b.** Epoxy with 5 wt.% PPE; **c.** Epoxy with 10 wt.% PPE.

3.2 Dynamic Mechanical Analysis (DMA):

The average values of four test specimens with a standard deviation of ±5% are presented in this section. The tan δ curves versus the temperature of the samples are shown in Figure 5a. The glass transition temperature (T_g) of the CF/Ep sample was obtained to be 68°C from the peak of the tan δ curve. With the addition of 5 wt.% of PPE into the matrix, the T_g of the composite increased by about 6°C, as observed in all PPE-modified samples (74°C). This shift in T_g is significant and is likely to have a positive influence on the thermo-mechanical properties of the composites. Both dissolution and interleaving methods of PPE addition resulted in the same level of T_g shift. Figure 5b and Figure 5c show the storage modulus (G′) and loss modulus (G″) curves of the samples, respectively. The G′ values of the samples showed a marginally decreasing trend with an increase in temperature (50°C to 80°C) and an increase in PPE content. The decrease in G′ and the increase in the tan delta peak values in the PPE-modified samples indicate that the incorporation of PPE particles might have influenced the network formation of the epoxy matrix during curing. It is due to the PPE molecules containing hydroxyl end groups, which are likely to react with the epoxy resin while curing and chemically bonded to the cross-linked epoxy network. These reactive modifications by PPE can influence molecular network formation, which can bring significant improvements in the overall performance of the composite. The loss modulus values of CF/Ep/PPE10-D and CF/Ep/PPE5-I (Figure 5c) were found to be higher than CF/Ep/PPE5-D samples. This behaviour might be due to the viscous regions caused by the accumulation of PPE particles and consecutive heat dissipation in the composites.
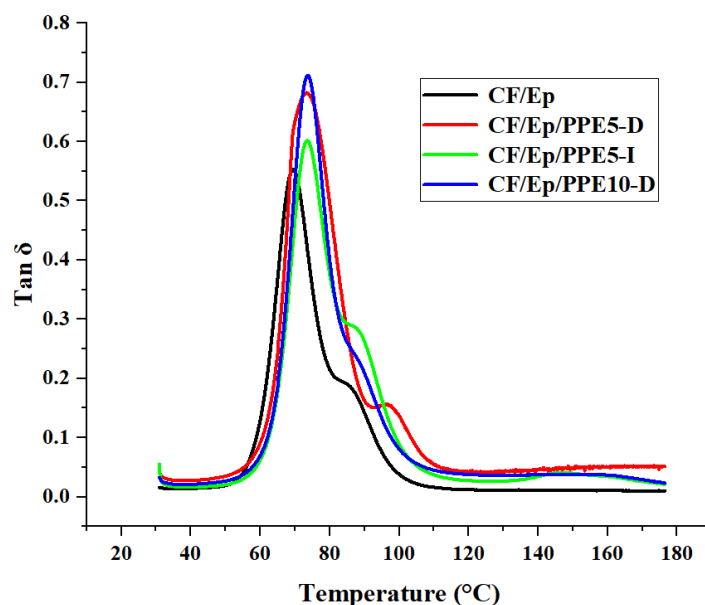

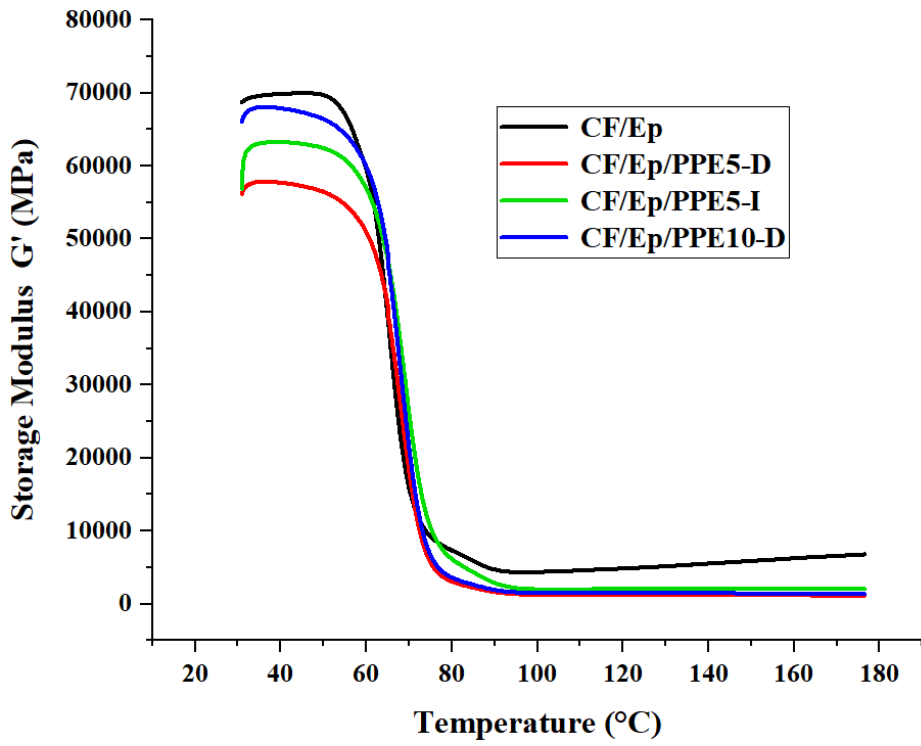Figure 5a: DMA curves; Tan δ versus temperature.

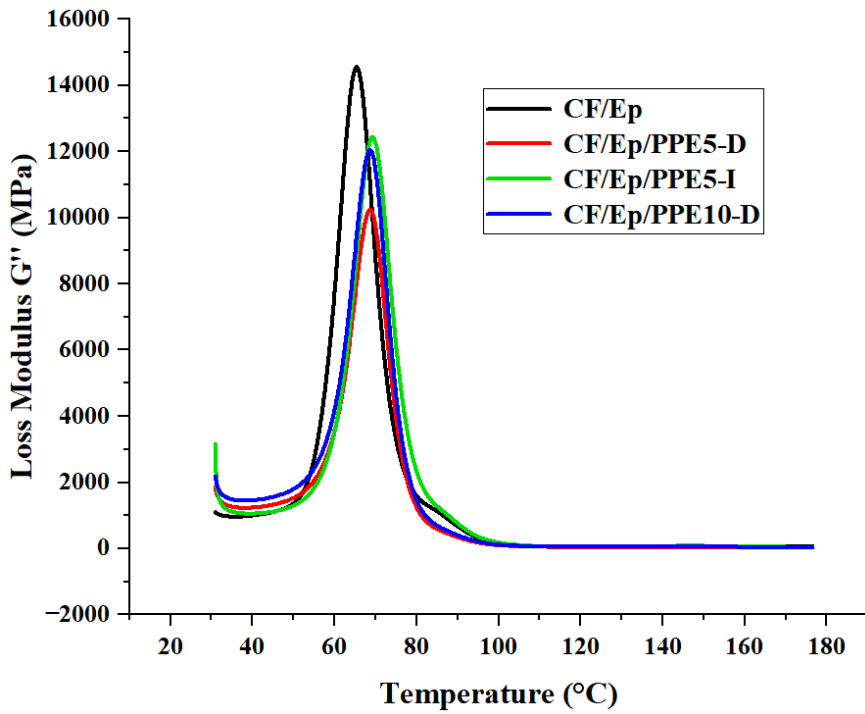Figure 5b: DMA curves; Storage modulus versus temperature.

Figure 5c: DMA curves; Loss modulus versus temperature.

3.3 Density

The average density of four specimens is presented in Table 1. The density of both carbon fiber (1.8 g/cc) and epoxy resin (1.15 g/cc) was comparatively higher than the toughening agent, PPE (1.03 g/cc). A considerable reduction in density was observed in PPE-modified samples compared to the unmodified ones. The decrease in density might be due to the presence of micro-voids in the modified matrix and also to the lower density (1.03−1.08 g/cc) of PPE compared to epoxy (1.15 g/cc). As the density variation is evident, it is likely to affect the final mechanical properties of the composites.

Table 1. Measured densities of different composite samples

Sample ID	Density (g/cc)
CF/Ep	1.5259
CF/EP/PPE5-D	1.4561
CF/EP/PPE5-I	1.4939
CF/EP/PPE10-D	1.4202

3.4 Mechanical properties

3.4.1 Tensile strength

The average tensile strength results of five test specimens of different composite samples are given in Table 2. The breaking loads of the samples were found to be minimally affected by the addition of PPE because fiber dominates in the longitudinal direction compared to the matrix. The variation in tensile strength and strain with increasing PPE content was found to be minimal. However, few literatures suggest that higher concentrations of PPE/PPO tend to alter the tensile strength. Tensile strength decreased from 64.9 MPa to 52.6 MPa for a DGEBA/20wt.% PPO [14] and 90 MPa to 85 MPa for a DGEBA/20wt.% PPO [15].

Table 2. Mechanical properties of composite specimens

Sample ID	Tensile strength (GPa)	Tensile modulus (GPa)	Tensile strain (%)	Density (g/cc)	Fiber fraction (volume %)
CF/Ep	1.15 ± 0.23	79.2 ± 4.4	1.07	1.5259	58 ± 0.8
CF/EP/PPE5-D	1.22 ± 0.14	80.5 ± 4.8	1.00	1.4561	57 ± 0.6
CF/EP/PPE5-I	1.03 ± 0.11	91.1 ± 7.2	0.93	1.4939	56 ± 1.3
CF/EP/PPE10-D	0.99 ± 0.15	89.9 ± 8.3	0.90	1.4202	56 ± 0.9

3.4.2 Mode-I fracture toughness:

A typical Mode-I fracture toughness (G_{IC}) test of a DCB specimen is shown schematically in Figure 6A. An actual sample picture taken from the digital image correlation (DIC) instrument during testing is shown in Figure 6B, mentioning details like pre-crack length (L_o) and actual crack length (L_c). The load versus displacement curves of all the samples are shown in Figure 7. The average G_{IC} values of the reference sample at the initiation and propagation zones were found to be 365 J/m^2 and 780 J/m^2, respectively. There was a significant improvement in the G_{IC} with the incorporation of PPE toughener. Ep/PPE10-D samples exhibited the highest G_{IC} value of 2054 J/m^2 in the initiation zone and 3740 J/m^2 in the propagation zone. The average G_{IC} values of six DCB specimens in each category of composite samples are presented in Table 3. Figure 8 shows the comparison of the R-curves of all the samples, indicating the average G_{IC} in the propagation zones.
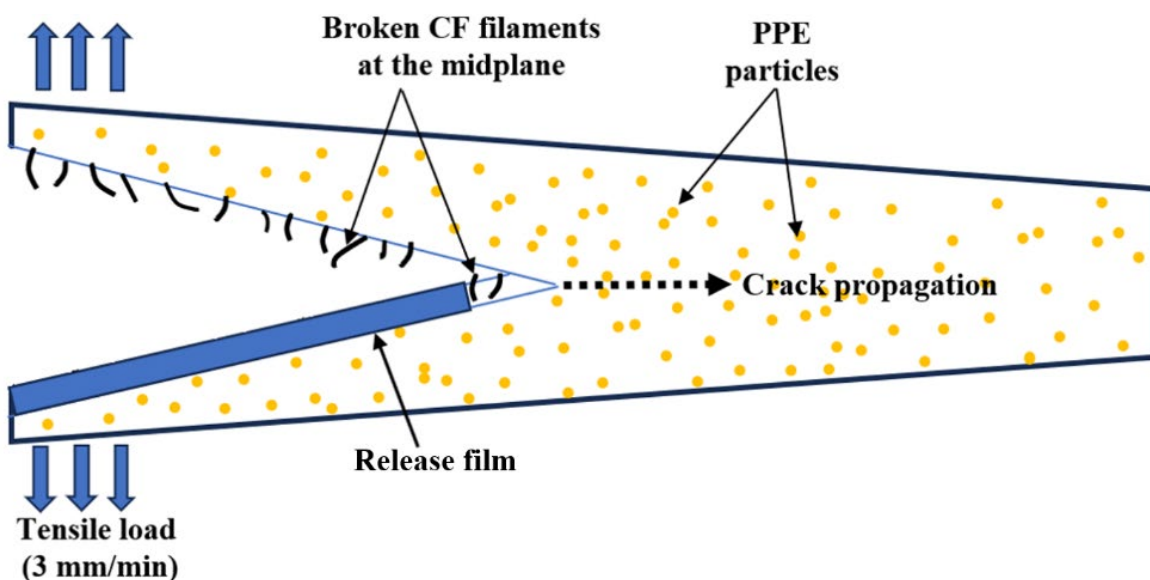

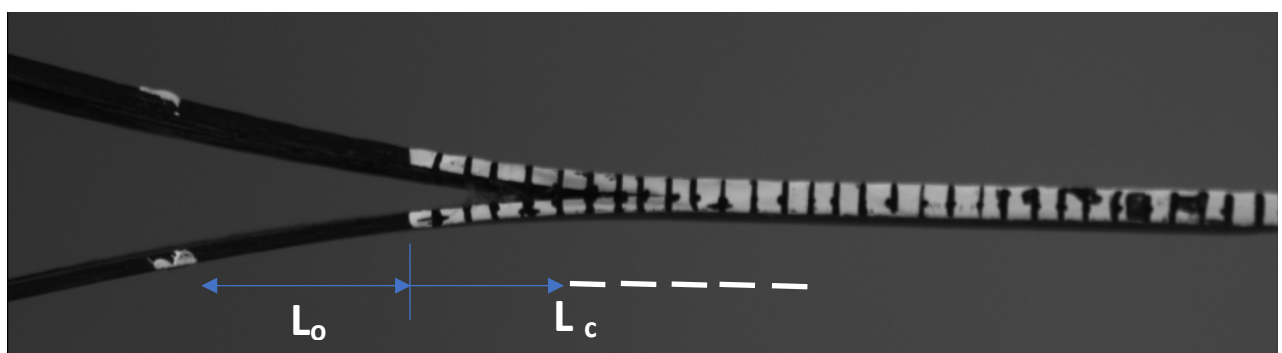Figure 6A. Schematic on visualization of DCB specimen test.

Figure 6B. Typical sample picture from DIC during Mode-I fracture toughness test.

Table 3. Interlaminar fracture toughness of different composite samples

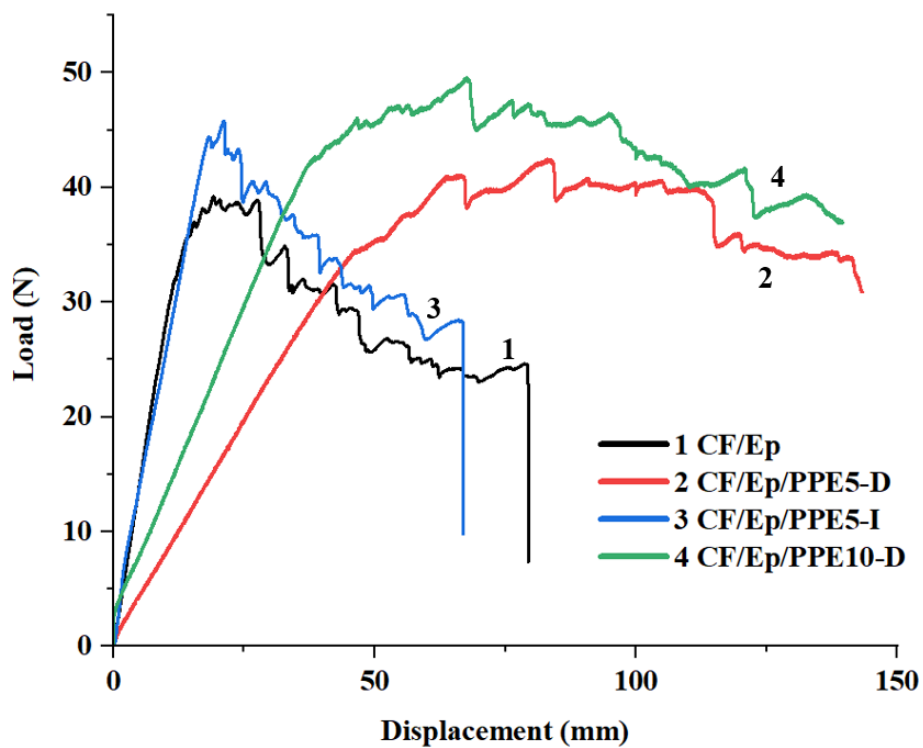| Sample ID	Mode-I Interlaminar Fracture Toughness G_{IC} (J/m^2)	
	Initiation	Propagation
CF/Ep (Reference sample)	365 ± 15	780 ± 42
CF/Ep/PPE5-D	696 ± 23	1248 ± 68
CF/Ep/PPE5-I	395 ± 28	1150 ± 76
CF/Ep/PPE10-D	2054 ± 107	3740 ± 345

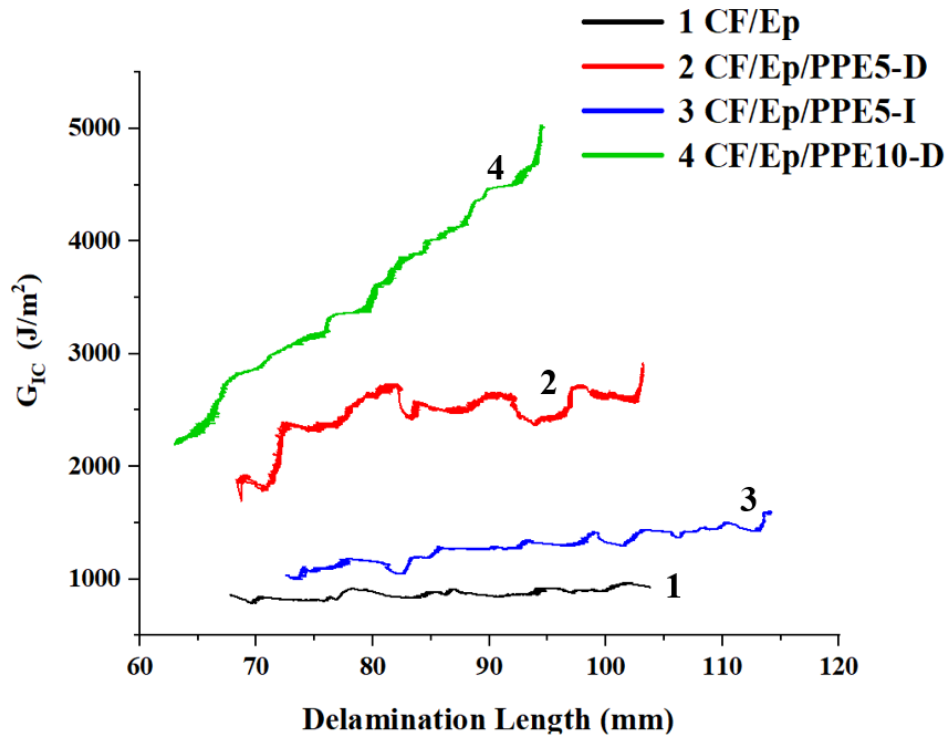Figure 7. Load versus displacement curves of all the samples.

14

Figure 8. Comparison of the R-curves (crack propagation) for different composite samples: 1) CF/Ep; 2) CF/Ep/PPE5-D; 3) CF/Ep/PPE5-I; 4) CF/Ep/PPE10-D.

The average G_{IC} propagation of the CF/EP/PPE5-I sample is higher than the unmodified sample but not as high as than that of the CF/EP/PPE10-D and CF/EP/PPE5-D samples. This could be due to the lower PPE content at the midplane, as the total amount of PPE was evenly distributed (one-third of 5 wt.%) at the interlaminar regions of the CF layers. It was observed that the dissolution method of PPE addition increased the G_{IC} propagation more effectively than the interleaving method and was found to be more promising. A homogeneous distribution of the PPE phase was generated within the epoxy matrix in the dissolution route that played an effective role in improving the fracture toughness (G_{IC}) of the sample. With the interleaving method, the PPE distribution per unit area was not uniform and the dissolution of PPE particles in liquid epoxy could happen for a very short time during the resin infusion process until the resin started to gel. Thus, the role of PPE as a toughener was less effective with the interleaving route, resulting in lower values of G_{IC}. When compared to the unmodified sample, about 3.2 and 4.8 times improvement were obtained in G_{IC} propagation for the CF/Ep/PPE5-D and CF/Ep/PPE10-D samples, respectively. The CF/Ep/PPE5-I sample resulted in 1.8 times higher G_{IC} with respect to the unmodified sample.

These results were encouraging and proved that the addition of PPE particles to the CF/epoxy composite can significantly increase the G_{IC} values. This is mainly due to its plastic deformation effect at the tip of the microcracks. The average G_{IC} values with error bars for the initiation and crack propagation zones are shown in Figure 9. It was also observed that the G_{IC} values did not change much with the partially agglomerated PPE particles and micro-voids in the sample, CF/Ep/PPE10-D. However, they made the resin mixture more viscous and significantly affected the vacuum resin infusion process.
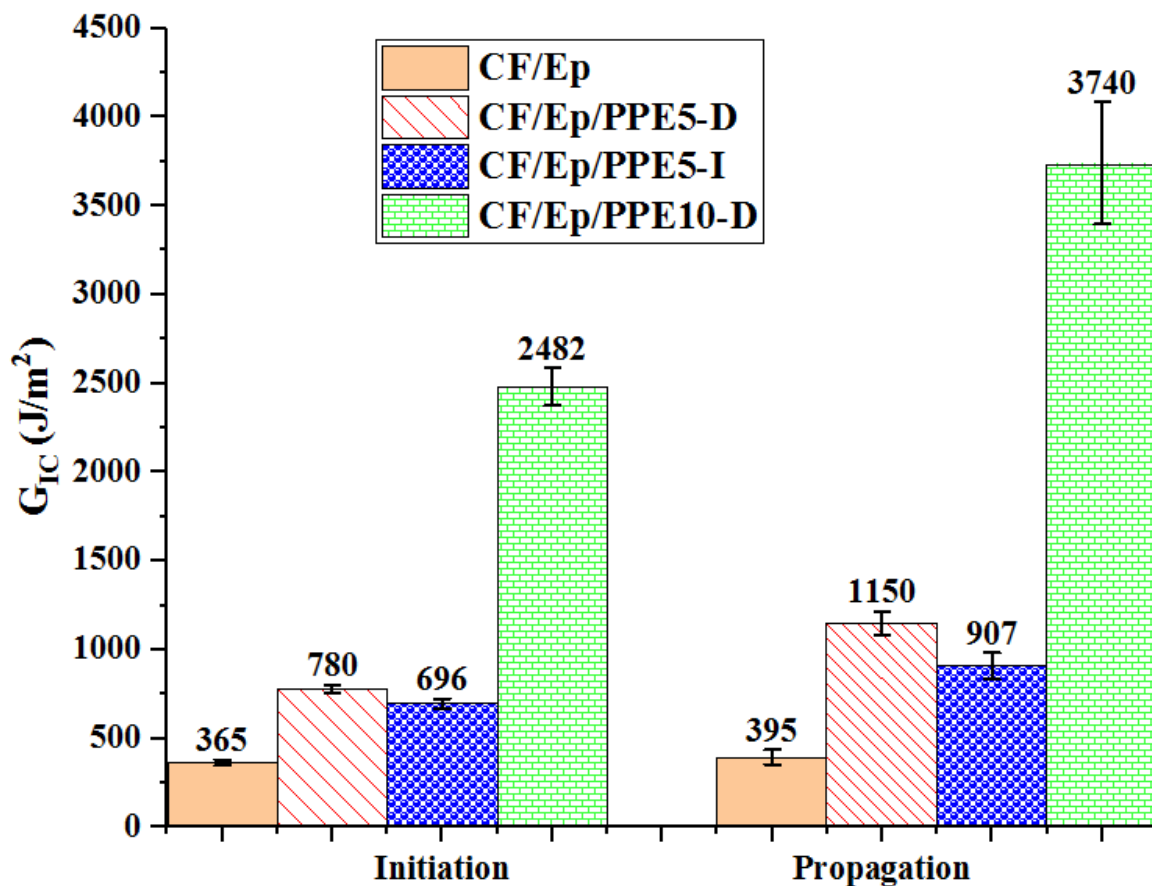

Figure 9. G_{IC} values for initiation and crack propagation zones in modified and unmodified CF/epoxy composite samples.

A literature survey about the effects of various toughening agents on the G_{IC} of CF/epoxy composite systems is presented in Table 4. The G_{IC} values obtained in this work with the incorporation of 5 wt.% and 10 wt.% PPE into the CF/epoxy composites are listed in the last row of Table 4, which showed a 191% and 380% improvement in G_{IC}, respectively, compared to the unmodified resin sample. This comparison emphasizes the significance of this work with similar toughening agents (PPO/PPE) and other tougheners such as PES, PEEK, PAEK,

phenoxy fibers, and rubber nanoparticles. The literature report by Y. Huan et al., [19] shows a 65% improvement in G_{IC} by incorporating 10 wt.% of PPE particles by the interleaving method. In this study, a 116% improvement in G_{IC} was shown for similar conditions (CF/Ep/PPE5-I), which is a significant and encouraging sign for further studies.

Table 4. Literature survey on G_{IC} values of CF/epoxy composites with different toughening agents

Composite system	Toughening agents	Mode-I G_{IC} (J/m^2)		Improvement	Literature Reference #
		Unmodified sample	Modified sample		
CF/epoxy composites interleaved with porous polyether sulfone films	PES (25 wt.%)	324	523	61.5 %	[13]
CF/epoxy (RTM6-2) composites, coating of poly (aryl ether ketone (PAEK) on carbon fiber	PAEK (20 wt.%)	261	751	188 %	[21]
CF/epoxy composites dissolved with Poly ether ether ketone (PEEK) as a toughener	PEEK	270	2250	733 %	[22]
CF/epoxy composites, Polyphenylene ether (PPO) particles were interleaved at the midplane of 16 layers stack of CF prepregs	PPO (10 wt.%)	131	216	65 %	[19]
CF/polybenzoxazine toughened with hydroxyl-terminated polyether sulfone (PES) by dissolution	PES (20 wt.%)	375	895	139 %	[24]

CF/epoxy composites with chopped phenoxy fiber added at the interlaminar regions of 4 CF fabric layers (400 mm × 370 mm)	Phenoxy fibers (5 cm; 10 wt.%)	271	700	158 %	[23]
CF/epoxy composites with electro spun Phenoxy fibers by dissolution and interleaving	Phenoxy fibers -Interleaving (1.6 wt.%)	500	2300	360 %	[25]
T-700 CF fabric / DGEBA epoxy composites interleaved with rubber nanoparticles and short carbon fiber	MX-153 rubber Nanoparticles (16 wt.%)	562	1724	207 %	[14]
CF/epoxy Prepreg of 200 gsm toughened with Electro spun PPO particles veils by interleaving	PPO (10 wt.%)	190	530	179 %	[26]
This experimental study Unidirectional CF fabric (603 gsm; 4 layers) /epoxy with PPE particles by dissolution and interleaving	PPE-D (5 wt.%) PPE-I (5 wt.%) PPE-D (10 wt.%)	780 780 780	1150 907 3740	191 % 116 % 380 %	--

3.5 Micromorphology (SEM)

Cross-sections of the composite samples were subjected to SEM analysis to investigate the epoxy resin impregnation through the CF fabric layers and the presence of micro-voids, if any. Figures 10 (a, b, c, d) show the SEM images of the cross-sectional specimens. The CF/Ep sample (Figure 10a) is fairly homogeneous, and there were no voids seen. In CF/Ep/PPE5-D and CF/Ep/PPE10-D (Figure 10b and 10d), a few micro-voids were seen that could be due to improper wetting resulting from the higher viscosity of epoxy resin with PPE particles. The CF/Ep/PPE5-I (Figure 10c) sample was relatively more heterogeneous and had more micro-voids. The possible reasons might be the non-uniform distribution of PPE particles in the interlaminar regions and friction due to the solid-solid interactions at the weaving edges of CF fabric layers. Similar DCB fracture surfaces are reported in the literature [27–29]. Huang et al., [20] have reported SEM images of CFRP DCB specimens made with 10 wt.% polyphenylene oxide (PPO) showing the PPO particle distribution between carbon fiber reinforcement.
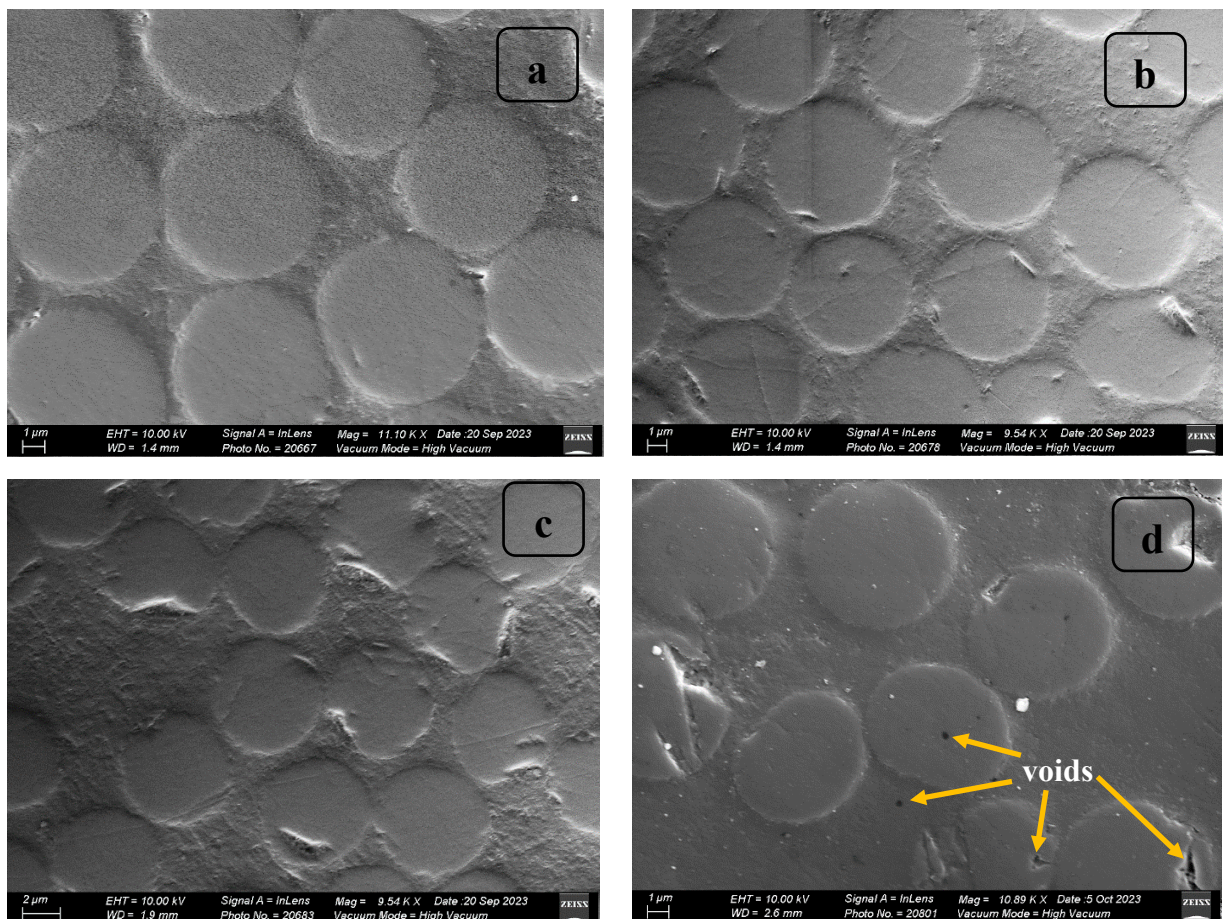

Figure 10. SEM images of cross-sections (a, b, c, d) of the CF/Ep, CF/Ep/PPE5-D, CF/Ep/PPE5-I, and CF/Ep/PPE10-D samples respectively.

4 Conclusions

This study aimed to enhance the interlaminar fracture toughness of carbon fiber/epoxy composites by incorporating a high-performance thermoplastic toughener (PPE). Carbon fiber/epoxy composites were fabricated using a vacuum-assisted resin infusion process with varied contents of PPE. The PPE particles were incorporated into the composites using two different techniques: dissolution and interleaving. DMA studies revealed that the addition of PPE increased the T_g of the CF/epoxy composites by about 6°C. There was a marginal decrease in the longitudinal tensile strength of the composite with the PPE addition. The cross sections of the laminates were examined under SEM, which showed adequate impregnation of epoxy resin across the thickness in the presence of micro-voids. The cross-sections of the samples CF/Ep/PPE5-I and CF/Ep/PPE10-D (Figures 10c and 10d) revealed similar morphological features that indicated agglomeration of the PPE phase, with 10 wt.% resembling PPE particles added in the interlaminar regions. The cross-sectional morphology of CF/Ep/PPE5-D was much more uniform, which implies 5 wt.% PPE is an optimum amount for dissolution in epoxy before the infusion process.

Adding PPE toughener yielded superior Mode-I fracture toughness (4-5 times; 3740 J/m2) compared to the unmodified sample. The PPE with hydroxyl end groups was very compatible with CF/epoxy composites, which provides a good choice of toughener for researchers. This experimental study showed that PPE is an effective thermoplastic additive to improve the fracture toughness of CFRP composites without compromising on either processability or glass transition temperature. While 10 wt.% PPE addition resulted in maximum G_{IC}, and the infusion process was easier with 5 wt.% PPE addition as the viscosity increase was less in this case. The experimental findings of this study will be useful for any future work in the field of thermoplastic toughened CFRP and can be explored for producing CF/epoxy prepregs. It is important to note that several chemicals, despite playing vital roles in industrial products, can have adverse effects on human health and the environment. Extreme caution and strict health and safety regulations are needed while using these chemicals. They should be replaced with equivalent biobased, more environmentally friendlier alternatives wherever applicable.

References

1. U.P. Breuer, *Commercial Aircraft Composite Technology*, Springer, 2016.
2. H. Nabipour, X. Wang, Y. Hu, Carbon fiber-reinforced composites based on an epoxy resin containing Schiff base with intrinsic anti-flammability, good mechanical strength, and recyclability, *European Polymer Journal* 2023, 194, 112166.
3. H. Rahmani, S.H.M. Najafi, S.S.Matin, A. Ashori, Mechanical Properties of Carbon Fiber/Epoxy Composites: Effects of Number of Plies, Fiber Contents, and Angle-Ply Layers, *Polymer Engineering and Science* 2014, 54, 2676-2682.
4. J. Zhang, G. Lin, U. Vaidya, H. Wang, Past, present and future perspective of global carbon fiber composite developments and applications, *Composites Part B* 2023, 250, 110463.
5. A.U. Sudhin, M. Remananb, G. Ajeesh, K. Jayanarayanana, Comparison of Properties of Carbon Fiber Reinforced Thermoplastic and Thermosetting Composites for Aerospace Applications, *Materials Today: Proceedings* 2020, 24, 453–462.

6. Y. Fu, Y. Zhang, H. Chen, L. Han, X. Yin, Q. Fu, J. Sun, Ultra-high temperature performance of carbon fiber composite reinforced by HfC nanowires: A promising lightweight composites for aerospace engineering, *Composites Part-B* 2023, 250, 110453.

7. J. Liang, L. Liu, Z. Qin, X. Zhao, Z. Li, U. Emmanuel and J. Feng, Experimental Study of Curing Temperature Effect on Mechanical Performance of Carbon Fiber Composites with Application to Filament Winding Pressure Vessel Design, *Polymers* 2023, 15, 982.

8. Q. Guan, L. Yuan, A. Gu, G. Liang, Fabrication of In Situ Nanofiber-Reinforced Molecular Composites by Non-equilibrium Self-Assembly. *ACS Appl. Mater. Interfaces* 2018, 10, 39293–39306.

9. Z. Zhang, K. Fu, and Y. Li Improved interlaminar fracture toughness of carbon fiber/epoxy composites with a multiscale cellulose fiber interlayer, *Composites Communications* 2021, 27, 100898.

10. D. Quan, G. Wang, G. Zhao, R. Alderliesten, On the interlayer toughening of carbon fiber/epoxy composites using surface-activated ultra-thin PEEK films, *Composite Structures* 2023, 303, 116309.

11. S.V. Heijden, L. Daelemans, B.D. Schoenmaker, I.D. Baere, H. Rahier, W.V. Paepegem, K.D. Clerck, Interlaminar toughening of resin transfer moulded glass fiber epoxy laminates by polycaprolactone electrospun nanofibers, *Composites Science and Technology* 2014, 104, 66–73.

12. L. Daelemans, S.V. Heijden, I.D. Baere, H. Rahier, W.V. Paepegem, K.D. Clerck, Nanofibre bridging as a toughening mechanism in carbon/epoxy composite laminates interleaved with electrospun polyamide nanofibrous veils, *Composites Science and Technology* 2015, 117, 244-256.

13. C. Cheng, C. Zhang, J. Zhou, M. Jiang, Z. Sun, S. Zhou, Y. Liu, Z. Chen, L. Xu, H. Zhan, Y. Muhuo, Improving the interlaminar toughness of the carbon fiber/epoxy composites via interleaved with polyether sulfone porous films, *Composites Science and Technology* 2019, 183, 107827.

14. Q. Chen, F. Wu, Z. Jiang, H. Zhang. J. Yuan, Y. Xiang, Y. Liu, Improved interlaminar fracture toughness of carbon fiber/epoxy composites by a combination of extrinsic and intrinsic multiscale toughening mechanisms, *Composites Part B* 2023, 252, 110503.

15. L. Luo, Y. Meng, T. Qiu, Z. Li, J. Yang, X. Cao, X. Li, Dielectric and Mechanical Properties of Diglycidyl Ether of Bisphenol A Modified by a New Fluoro-terminated Hyperbranched Poly(phenylene oxide), *Polymer Composites* 2013, 34, 1051-1060.

16. J. Lv, Y. Meng, L. He, T. Qiu, X. Li, H. Wang, Novel Epoxidized Hyperbranched Poly(phenylene oxide): Synthesis and Application as a Modifier for Diglycidyl Ether of Bisphenol A, *J. Appl. Polym. Sci*. 2013, 128, 907-914.

17. T.K.L. Nguyen, S. Livi, B.G. Soares, H. Benes, J.F. Gerard, J.D. Rumeau, Toughening of Epoxy/Ionic Liquid Networks with Thermoplastics Based on Poly(2,6-dimethyl-1,4-phenylene ether) (PPE), *ACS Sustainable Chem. Eng*. 2017, 5, 1153−1164.

18. Q. Guan, L. Yuan, A. Gu, and G. Liang, Fabrication of In Situ Nanofiber-Reinforced Molecular Composites by Non-equilibrium Self-Assembly, *ACS Applied Materials & Interfaces* 2018, 10, 39293−39306.

19. Y. Huang, W. Liu, Q. Jiang, Y. Wei, and Y. Qiu, Interlaminar Fracture Toughness of Carbon-Fiber-Reinforced Epoxy Composites Toughened by Poly-(phenylene oxide) Particles, *ACS Applied Polymer Materials* 2020, 2, 3114−3121.

20. L. Weng, Y. Zhang, X. Zhang, L. Liu, H. Zhang, Synthesis and Properties of Cured Epoxy Mixed Resin Systems Modified by Polyphenylene Oxide for Production of High-Frequency Copper Clad Laminates, *Polymer Composites* 39 (2018) E2334-2345.

21. Z. Wu, X.S. Yi, A. Wilkinson, Interlaminar fracture toughness of carbon fiber/RTM6-2 composites toughened with thermoplastic-coated fabric reinforcement, *Composites Part B: Engineering*, 2017, 130, 192-199.

22. S. Hashemi, A. J. Kinloch, J. G. Williams, The analysis of interlaminar fracture in uniaxial fiber-polymer composites, *Proc. R. Soc. Land*. A 1990, 427, 173-199.

23. W.Y. Wong, L. Lin, P.T. McGrail, T. Peijs, P.J. Hogg, Improved fracture toughness of carbon fiber/epoxy composite laminates using dissolvable thermoplastic fibers, *Composites Part A: Applied Science and Manufacturing*, 2010, 41, 759-767.

24. B.D.S. Orozco, D. Roy, A. Kervennic, P. T. McGrail, W. F. Stanley, Toughening of carbon fiber/polybenzoxazine composites by incorporating polyethersulfone into the interlaminar region, *Materials & Design* 2016, 93, 297-303.

25. H. Zhang, A. Bharti, Z. Li, S. Du, E. Bilotti, T. Peijs, Localized toughening of carbon/epoxy laminates using dissolvable thermoplastic interleaves and electro spun fibers, *Composites Part A: Applied Science and Manufacturing* 2015, 79, 116-126.

26. Y. Huang, Y. Qiu, Y. Wei, Composite interlaminar fracture toughness imparted by electrospun PPO, veils and interleaf particles: A mechanistic comparison, *Composite Structures* 2023, 312, 116865.

27. D.C. Hartlen, J. Montesano, D. S. Cronin, A Composite Rigid Double Cantilever Beam Specimen for Assessing the Traction–Separation Response of Mode-I Delamination in Composite Laminates, *Experimental Mechanics* 2023.

28. V. Srinivasa, V. Shivakumara, V. Nayaka, S. Jagadeeshaiaih, M. Seethram, R. Shenoy, A. Nafidi, Fracture Morphology of Carbon Fiber Reinforced Plastic Composite Laminates, *Materials Research* 2010, 13, 417-424.

29. M.A.A. Mohsin, L. Iannucci, E.S. Greenhalgh, Delamination of Novel Carbon Fiber-Based Non-Crimp Fabric-Reinforced Thermoplastic Composites in Mode I: Experimental and Fractographic Analysis, *Polymers* 2023, 15, 1611.